# Analyst

## Accepted Manuscript

This article can be cited before page numbers have been issued, to do this please use: R. Buiculescu, D. Stefanakis, M. Androulidaki, D. Ghanotakis and N. A. Chaniotakis, *Analyst*, 2016, DOI: 10.1039/C6AN00783J.

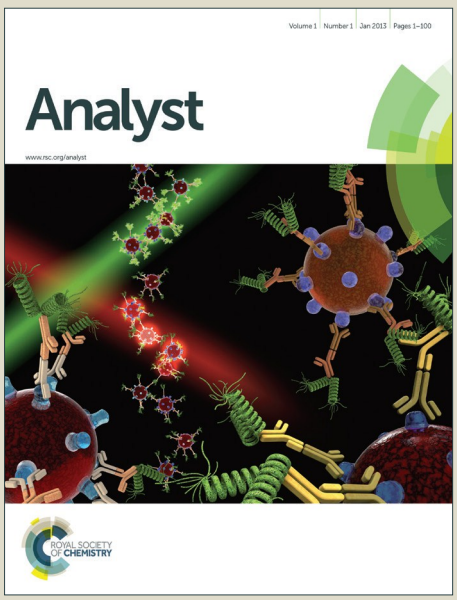




ROYAL SOCIETY OF CHEMISTRY

www.rsc.org/analyst

# Controlling Carbon Nanodot Fluorescence for Optical Biosensing

*Raluca Buiculescu[1], Dimitrios Stefanakis[2], Maria Androulidaki[3], Demetrios Ghanotakis[2], Nikos A. Chaniotakis[1]*

[1] Laboratory of Analytical Chemistry, Department of Chemistry, University of Crete, Heraklion, 73001 Crete, GREECE,

[2] Laboratory of Biochemistry, Department of Chemistry, University of Crete, Heraklion, 73001 Crete, GREECE,

[3] Microelectronics Research Group, IESL-FORTH, P.O. Box 1385, Heraklion 71110, Crete, GREECE

Corresponding Author: Tel: +302810545018, Fax: +302810545165; E-mail: chaniotakis@uoc.gr





## *ABSTRACT*

In this work we report on the optical properties of specific synthetic carbon nano-dots (CDs) and their suitability for the development of optical biosensors. We examine the photoluminescent behavior of these CDs under different conditions, in their native form, as well as when conjugated to the catalytic protein glucose oxidase (GOx) for the construction of the optical glucose biosensor. The effect of pH and hydrogen peroxide on the observed spectra is examined as the basis for the biosensor development. The CDs examined here have inherent surface amino carboxyl functional groups which allow for easy conjugation to biomolecules via EDC-NHS, providing a well defined platform for biosensing applications. We conclude that the well controlled, stable, and highly efficient fluorescence behavior of the CDs in solution or in conjugate provide the grounds for this class of materials to be used in a variety of arrangements for the development of optical and optoelectrochemical detection systems.

## *KEYWORDS*

Carbon nano dots, photoluminescence, fluorescence, optical biosensor, glucose oxidase

## *INTRODUCTION*

Quantum nano-sized structures have played a decisive role in the development of novel highly sensitive detection technologies during the last couple of decades. Semiconductor quantum dots[1,2], gold nanoparticles[3] and carbon nanostructures[4,5] have constituted the major players in this field. The on going development of novel nanostructures provides the scientific community with new possibilities for ultra sensitive, direct, selective and *in-vivo* detection schemes.

The past decade, a new class of carbon based materials with fascinating properties and potential applications has emerged[6,7,8,9], namely carbon nanodots (CDs). They are discrete[8,10] quasi-spherical nanoparticles with diameters ranging from 2 to 30 nm and excitation wavelength ($\lambda_{ex}$) dependent fluorescence[6,11]. CDs have both chemical and physical characteristics that are different from semiconductor-based QDs. In particular, they are less expensive and easier to synthesize[8,12,13], are not toxic[12], and are considered biocompatible[6,7,8,13,14], while their surface carries large amounts of oxygen or nitrogen containing functional groups[6,9]. These functionalities furnish CDs with characteristics such as controlled water solubility and suitability for further chemical functionalization[15]. This lead to an exponential increase in their applications extending to a variety of categories, such as optical bioimaging[6,16], biosensing[17,18,19] and sensing applications in biomedicine such as drug/gene delivery[20,21], anticancer agents antibacterial[22] or antioxidant activity[23].

In general, the term CDs describes various nanosized carbon materials with one dimension less than 10 nm. The synthetic route and the starting materials will provide CDs with different characteristics, sizes, internal structure, and edge functionalities. In particular, the hybridization and oxidation state of the edge carbon atoms can be in a $sp^2$ or $sp^3$ hybridized state, with mainly oxygen or nitrogen edges. Based on these characteristics, one can have Graphene Quantum Dots (GQDs), anisotropic nanoparticles consisting of one or a few layers of graphene, with lateral dimensions larger than their height, and spherical Carbon Nano Dots (CNDs). These CNDs are subdivided into Carbon Nanoparticles (CNPs) which do not have a crystal lattice, and Carbon Quantum Dots (CQDs), which have a crystal lattice[24].

For these reasons, the synthetic method to be used depends on the specific application. The type, size, shape, outer functionalities as well as the quality of the CDs final product will be determined during synthesis. There are two main synthetic routes being followed, the top-down synthesis for applications in optoelectronics, semiconductor etc., and the bottom-up synthesis for applications in bio-chemistry.

It has already been described that the observed fluorescence of the CDs is size and capping dependent 6,[25,26,27,28]. At the same time there have been numerous reports describing that selective ion recognition of the surface of semiconductor QDs can influence the observed fluorescence, and thus QDs can be used as optodes for selective ion detection2. Grafting chemical recognition functionalities onto CDs could result in the same optical sensing behavior and it is thus expected that CDs fluorescence can be influenced by the surrounding environment. In this case, the peripheral functionalities could be custom tailored for selective chemical and biological recognition. Grafting specific chemically sensitive functionalities onto CDs has been achieved so far with two methods: either by embedding them within the CDs during synthesis or in a later step by covalent binding to their surface functionalities[13,29]. Both these methods allow the control of the chemical recognition characteristics of the CDs, while at the same time offering better solvent compatibility and solubility.

Such functionalized CDs can provide the scientific community with a new and highly promising optical recognition platform, which can be implemented in a wide area of applications. Due to their biocompatibility, CDs are emerging as viable alternatives to current nano- and quantum materials such as semiconductor quantum dots, gold and silver nanocrystals, fullerenes, carbon nanotubes and nanofibers[30,31,32,33]. For this reason CDs technology holds a great potential for *in-vivo* bioanalysis and bio-sensing. For these applications to be realized, relating the physicochemical activity of the functional surface agents to the optical properties of the CDs is of paramount importance.

The absorption of the electromagnetic radiation of CDs is controlled by the C-C conjugation, as well as any absorbing moieties found or added to their surface. Based on the existing knowledge of the inner structure of the CDs, their absorption is based on the graphene structure (phenyl moieties), and is expected to be in the range between 230 to 320 nm ascribed to the π–π* transition of aromatic C–C bonds. Higher absorption frequencies are attributed to the n–π* transition of C=O bonds or other connected groups[34]. However, the absorbance of CDs is expected to change to longer wavelength upon surface modification, due to possible disruption of some of the $sp^2$ hybridization within a few atomic layers of its surface. This absorption change is also expected to have an effect on both the CDs QY, as well as the PL peak position.

There are a number of PL mechanisms that have been suggested, albeit, the exact mechanisms of the CDs PL will depend on the material, and thus a very careful investigation is required before any conclusion as to its origin can be made. Photoluminescence intensity is sensitive with laser power and wavelength ($\lambda_{ex}$). This is most probably due to the size distribution of the CDs, since the quantum effect is strongly affected by the nanoparticle size. In addition, their PL is

influenced by the surface moieties, as well as their chemical state (i.e. protonation state, oxidation condition, as and O/N ratios). The type of functionalities on the surface, as well as their state can act as different energy traps, whose emission is altered significantly upon change of their state, similar to that shown in other nanocrystals[35]. The PL intensity of the CDs is also pH dependent[36,37,38] and is expected to change upon pH changes, but there is no clear trend reported as of yet that will relate these two values. The peak shift should also be considered here, since a shift is very plausible upon changes in pH values.

As an application of the newly synthesized and well-characterized CDs, we conjugated them with glucose oxidase (GOx) and describe here an optical glucose biosensor. The CDs synthesis is fast, easy, and produces particles with amino functional groups on their surface, allowing for easy conjugation to biomolecules. The active enzyme is then covalently conjugated onto the surface of the CDs and the obtained CDs – GOx complex is being evaluated by monitoring the effect of the enzyme's substrate, glucose.

## *EXPERIMENTAL*

### Materials

L-Arginine monohydrochloride, 4,7,10-trioxa-1,13-tridecanediamine (TTDDA), N-ethyl-N'-(3-dimethylaminopropyl) carbodiimide (EDC), N-hydroxysulfosuccinimide sodium salt (NHS), multi walled carbon nanotubes (MWCNTs – OD=3-10nm, ID=1-3nm, length=0.1-10μm, >90%) and fullerene C-60 (99.5%) were obtained from Sigma-Aldrich. Graphene oxide monolayer powder (GO) was purchased from NanoInnova Technologies. Glucose oxidase (GOx) from *Aspergillus niger* was obtained from Fluka. All salts used were of analytical grade and purchased from Sigma-Aldrich. All buffer solutions were prepared using ~18 MΩ-cm$^{-1}$ nanopure water (EASY pure model D7033, Barnstead).

### Synthesis of CDs

CDs were prepared by modifying an already published method[39]. Briefly, L-arginine monohydrochloride (Arg) and the capping agent, TTDDA, were mixed at a ratio of 3:1 with the aid of 2mL nanopure water. The mixture was placed in a 100mL round-bottom flask and was subjected to microwave assisted pyrolysis in a microwave oven at 800W for exactly 40 seconds. Longer pyrolysis times lead to the compounds of the mixture being completely burned off. During this process, water rapidly starts to boil and eventually evaporates leaving on the bottom of the flask a dark colored viscous solution. This procedure results in CDs with amino functionalities on their surface.

View Article Online
DOI: 10.1039/C6AN00783J

## Purification of CDs

The microwave obtained product was firstly filtered through a 0.2-μm pore size filter to remove the larger aggregates and then purified by gel filtration chromatography. A column packed with Sephacryl s-200 was used to separate the unreacted molecules from the CDs, where ultrapure water consisted the mobile phase. The elutions were characterized by UV-Vis and fluorescence spectroscopy.

## Characterization of CDs

For photoluminescence (PL) measurements, a CW He-Cd laser was used with nominal power 35mW at 325nm excitation wavelength. All the spectra were recorded by a very sensitive $LN_2$ cooled CCD camera at room temperature. The C60, GO and MWCNTs were analyzed in powder form, while the CDs were measured as synthesized, in aqueous solution.

Solution absorbance spectra were recorded on a Shimadzu UV-2700 spectrophotometer.

High-resolution transmission electron microscopy (HR-TEM) images of CDs were obtained using a JEOL JEM-2100 Electron Microscope, operating at 80kV. The samples were prepared by evaporation of droplets placed on Formvar/Carbon coated TEM grids (Analytical Instruments S.A.). The solvent was allowed to evaporate under atmospheric conditions.

The Surface Enhances Raman Scattering (SERS) spectra were recorded on a Nicolet Almega XR Raman spectrometer with a long distance 50x objective lens and 780nm excitation laser at 40mW operating at high resolution. The experiments were performed by depositing two consecutive layers of a silver particles solution and of the Arg-TTDDA CDs solution on an EZ-Spot Micro Mount sample slide (Thermo Fisher Scientific). The first layer (silver particles) was allowed to dry at room temperature for one hour before deposition of the second layer (CDs) took place.

Silver particles appropriate for the SERS experiments were obtained by the chemical reduction of silver nitrate by trisodium citrate[40]. The citrate induced reduction of silver nitrate produces a grayish solution with an absorption band with maximum at 420nm. The greenish-yellow suspension of silver particles was purified by centrifugation at 15,000g for 3 min and the precipitate was washed twice with nanopure water.

The ATR-FT-IR spectra were recorded on a Thermo-Electron Nicolet 6700 FT-IR optical spectrometer with a DTGS KBr detector at a resolution of $2cm^{-1}$.

View Article Online
DOI: 10.1039/C6AN00783J



## Conjugation of CDs with GOx

Freshly synthesized CDs were conjugated with GOx through the coupling reaction of EDC and sulfo-NHS. EDC is one of the most used cross-linking agents to couple carboxyl groups to primary amines. It reacts with a carboxyl group to form an amine-reactive *O*-acylisourea intermediate that further, upon addition of sulfo-NHS, produces a semi-stable amine reactive NHS ester. EDC and NHS (20mM stock solutions) were mixed with a 20mg/mL GOx stock solution and brought to a final volume of 4mL with $KH_2PO_4$ buffer (pH 6.0, 50mM) and vortexed for 45 minutes. CDs were added to the mixture and vortexed for another 60 minutes. At the end of the conjugation procedure, the mixture was filtered by centrifugation on a 50.000 MWCO filter, at 4$^o$C and 5000 rpm, for 7 minutes. The supernatant containing the newly formed CDs – GOx conjugates was washed twice on the same filter with $KH_2PO_4$ buffer and finally kept at 4$^o$C for further experiments.

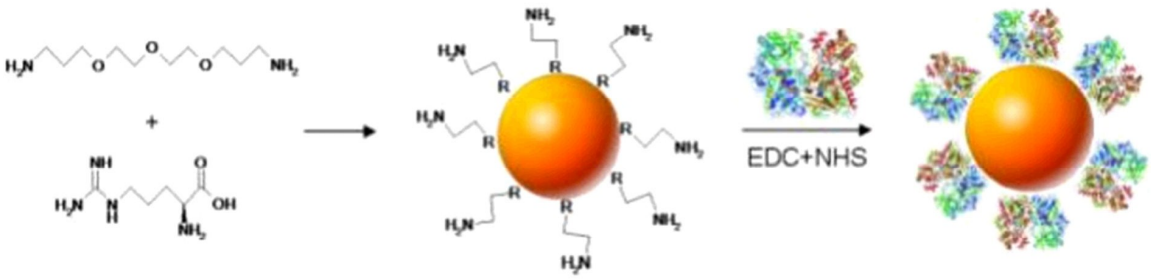


**Figure 1.** Schematic of the GOx – CDs conjugation process

## CD-GOx activity measurements

The enzyme GOx catalyses the oxidation of glucose to hydrogen peroxide and D-glucono-δ-lactone. GOx is a dimeric globular protein consisting of two 80kDa subunits, with an overall dimension of 6.0x5.2x7.7nm$^3$ and an FAD molecule non covalently but tightly bound to the active site of each of the two subunits.

The concentration of the free and immobilized GOx was measured using the Bradford method[41].

For the determination of the kinetic parameters, an YSI Model 5300 biological oxygen monitor was used to follow the oxygen consumption by GOx enzyme. The method utilizes Clark type polarographic oxygen probes immersed in a magnetically stirred sample chamber.

The SDS /PAGE electrophoresis was performed according to the Laemmli method using a self-built system consisting of 10% acrylamide gels. Staining was carried out with 0.02% Coomassie Brilliant Blue G-250 in 10% acetic acid[42].

### Fluorescence measurements

Quartz Suprasil optical cuvettes for fluorescence measurements (light path 10mm) were obtained from Hellma and the fluorescence spectra have been recorded on a Lumina Fluorescence Spectrometer (Thermo Scientific) equipped with a 150W CW Xenon-arc lamp. All samples were analyzed at room temperature.

For the pH assay, a range of solutions of different and precisely controlled pH values from 3.98 to 11.93 were prepared, mixed with the same amount of CDs and left to incubate for 10 min before recording their fluorescence intensities. The pH solutions were prepared by adding various amounts of KOH (1.0M) or HCl (1.0M) to a MES -buffered solution (0.1 M, pH 4.50).

For the hydrogen peroxide ($H_2O_2$) assay, the CDs were mixed with various amounts of $H_2O_2$ to reach final concentrations from $10^{-9}$ to $10^{-1}$ M and left to incubate for 10 min before recording their fluorescence.

For the glucose assay, 5μL of the CDs – GOx conjugates were mixed with different amounts of the glucose (stock solution 5mM) and diluted to 1500μL with $KH_2PO_4$ buffer. The mixtures were incubated for 10 min and their fluorescence was subsequently recorded at an excitation wavelength of 325nm.

## *RESULTS AND DISCUSSION*

Our synthesis approach is rapid, facile and renders CDs with different functionalities onto their surface depending on the reagent to be used. We have used 4,7,10-trioxa-1,13-tridecanediamine which renders CDs with amino-terminated functionalities for further conjugation with the enzyme of interest. The morphology of the newly obtained CDs was determined by means of HR-TEM and a micrograph is shown in Figure 2a. The image reveals the formation of particles of a few sizes, mainly square – shaped with rounded corners. The size distribution of the nanoparticles as measured from the TEM image is in the order of 13.2±2.0nm. The range of the sizes was obtained by measuring the diameter of 106 nanoparticles and it is shown in the histogram presented in Figure 2b. It should be mentioned here that as it can be seen from Figure 2a, there are cluster formation on the TEM grid. This clustering is crucial in the evaluation of the

PL spectra that follow, as it has been observed that this is a concentration dependent phenomenon.

View Article Online
DOI: 10.1039/C6AN00783J

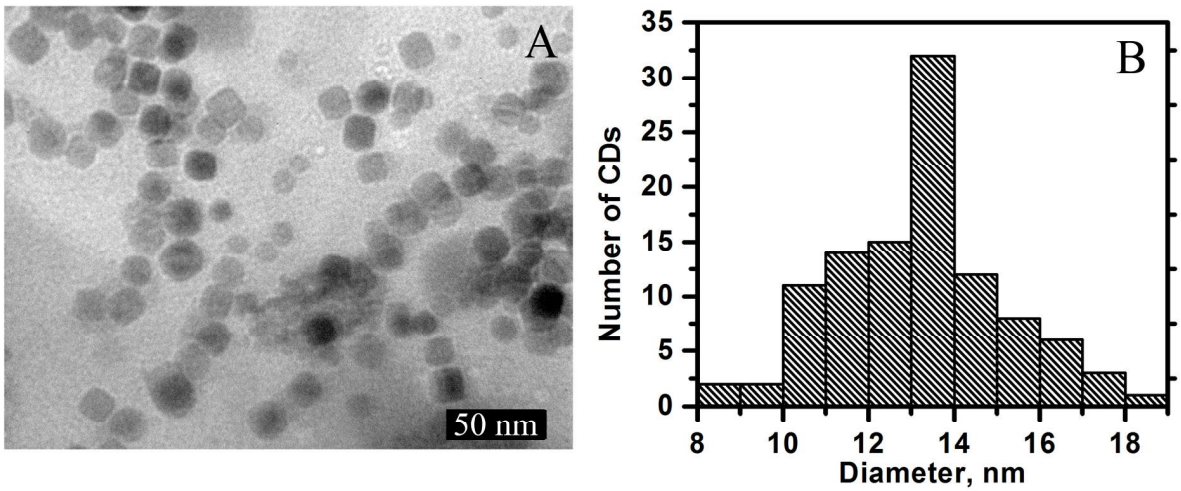


**Figure 2.** HR-TEM image of CDs (a) and their respective histogram (b).

The newly synthesized CDs can be excited over a wide range of wavelengths (260-350nm) as it can be seen in Figure 3. Their peak is shifting slightly towards higher wavelengths with increase of the excitation wavelength, but with the highest intensity peak being registered with excitation at 295nm (Figure 3a). Due to the fact that GOx has also intense fluorescence when excited with wavelengths below 310nm (Figure 3b), we have chosen for all further experiments, an excitation wavelength of 325nm in order to avoid enzyme interference.

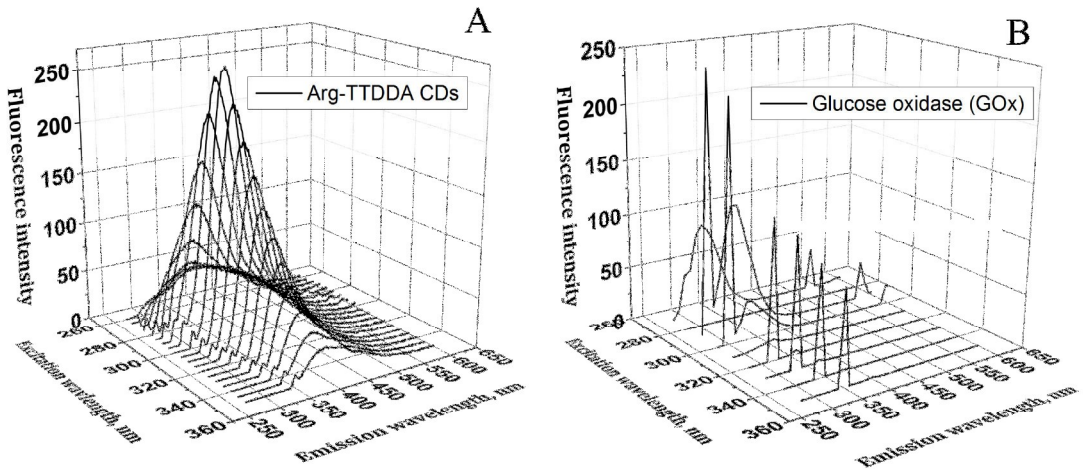


**Figure 3.** The 3D excitation-emission of CDs (a) and of GOx (b)

The dependence of the emission peak on the excitation wavelength is typical for CDs behavior. This phenomenon can be due to the optical characteristics of CDs with different diameter nanoparticles, and/or to different emissive traps that exist on the CD surface. In addition, the existence of a limited number of chromophores inside the CDs' sphere is likely the cause of this 'localized' feature[9].

The optical properties of the CDs were subsequently compared to a series of carbon based nanomaterials that have been used previously for biosensor development, namely fullerenes C60[43,44], graphene oxide (GO)[45,46] and multi walled carbon nanotubes (MWCNTs)[47,48]. The PL spectra of the carbon compounds are shown in Figure 4a.

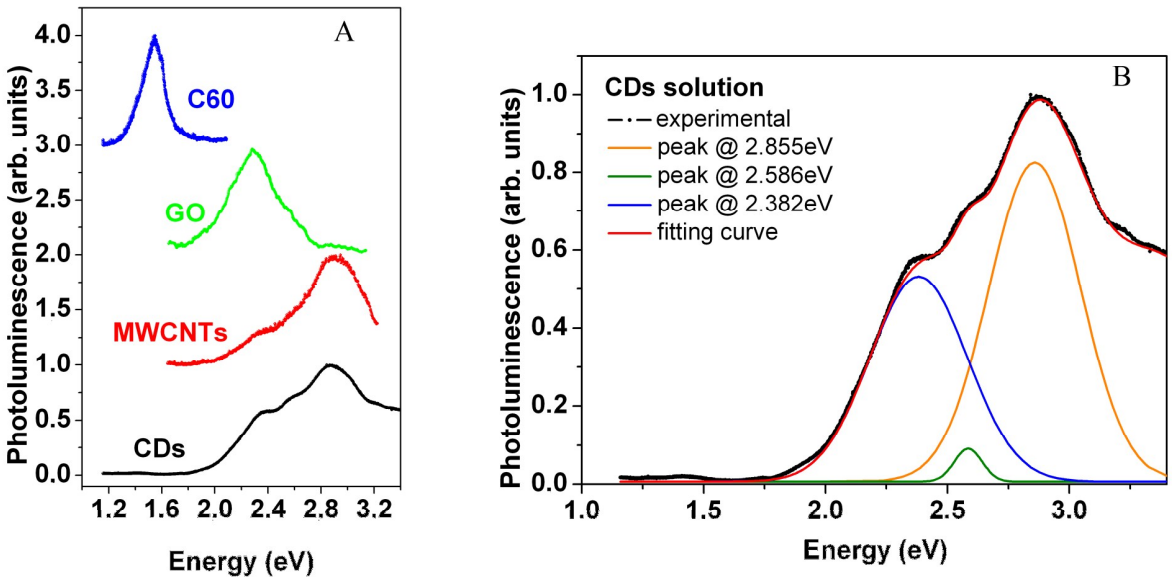


**Figure 4.** Room temperature PL of C60, GO, MWCNT and CDs solution (a) and the deconvolution of the CDs spectrum (b).

As it is observed, all carbon materials show relatively broad PL peaks and similar integration PL intensities, with the exception of the CDs solution whose integration intensity is approximately 100 times higher. In addition to the measured spectra, a Gaussian function[49,50,51] is used to fit this data, and to deconvolute the spectra peaks (Figure 4b) with values presented in Table 1:

**Table 1: Peak energy, width, and intensities of carbon nanomaterials.**

| | E (eV) | FWHM (meV) | Total Integration Intensity (a.u.) |
|---|---|---|---|
| C60 | 1.526 | 240 | 115 |
| GO | 2.291 | 435 | 205 |
| MWCNTs | 2.920 | 505 | 523 |
| CDs | 2.855<br>2.382<br>2.586 | 432<br>469<br>135 | 28497 |

As shown in Figure 4a, different carbon nanostructures have distinct PL spectra shapes, as well as energy distributions. While fullerene-C60 show a well defined, Gaussian distribution at 1.526eV, GO has an almost double FWHM and higher band gap energy at 2.29eV. Both MWCNTs and CDs have a more complex spectrum. This is to be expected, since both of these materials are not so well defined, and have a wide size distribution, as described above. In particular, the deconvolution of the CDs spectrum (Figure 4b) shows clearly the existence of three peaks at 2.382, 2.586 and 2.855eV. Upon close examination, the peak at 2.586eV is unique to the CDs, since it does not appear in any of the other carbon nanomaterials. Further purification of the CDs will provide dots with narrower size distribution, and thus highly fluorescent carbon nanoparticles with distinct and narrow emission wavelengths covering a wide range of the visible spectrum. This procedure is thus mandatory if CDs are to be used in demanding optoelectronic applications.

Raman spectroscopy, a non-destructive tool which allows for the observation of different types of bonding vibrations, was used to study the morphology of the CDs synthesized. It is the method of choice for the precise quantification of $sp^2$ and $sp^3$ hybridized carbon ratios within the carbon based material. Carbon nanostructures have characteristic D ($sp^3$-hybridized) and G ($sp^2$-hybridized) bands which are indicative of the extent of defects existent in the structure and of the in-plane bond-stretching motion of pairs of $sp^2$ C atoms[52] respectively, as well as the possible oxidation state of the carbon on the surface of the material.

Our attempts to collect Raman spectra for CDs either in solid form or in solution, resulted in strong fluorescence emission, even with NIR excitation at 780 nm, which overwhelmed any possible Raman features. For this reason, we proceeded with Surface-Enhanced Raman

Spectroscopy (SERS) with the use of silver (Ag) particles. SERS is a very valuable Raman method since it provides a 3 to 7 orders of magnitude enhancement in the intensity of the Raman signal[53]. In this way, highly sensitive analysis is achieved, while peaks otherwise obscured by the background, are clearly visible.

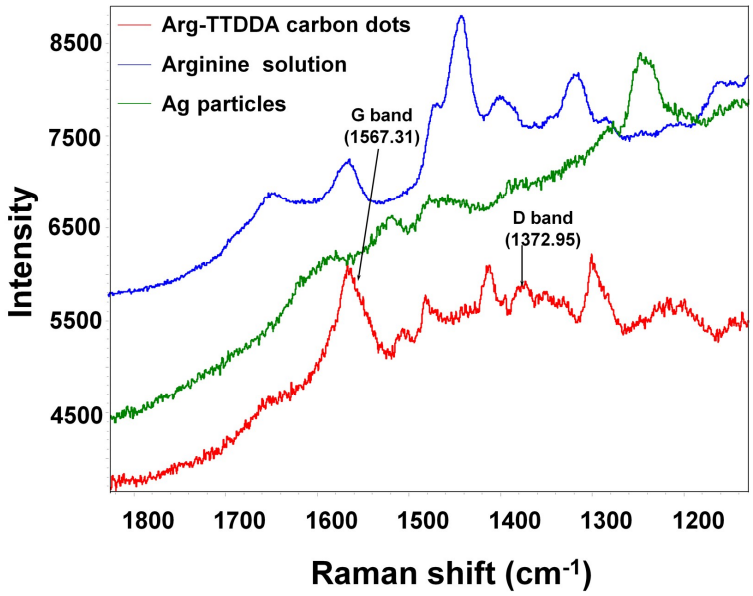


**Figure 5.** SERS spectra of the Arginine background (blue line), plain Ag particles (green line), and the Arg-TTDDA CDs (red line)

Figure 5 shows the SERS spectra of CDs, of arginine solution and of the plain Ag particles, for comparison reasons. The spectrum of the Ag particles is relatively smooth showing only one peak at 1247cm$^{-1}$ which is attributed to the vibration of the citrate skeleton. The spectrum of the CDs contains the two signature peaks mentioned earlier, namely the D band at 1372.95cm$^{-1}$ and the G band at 1567.31cm$^{-1}$. As has been explained before[37], the D band is associated with vibrations of the edge carbon of graphitic or glassy carbon. While this band is pretty weak and due to the background noise it can not be clearly distinguished, the G band peak, which corresponds to the $E_{2g}$ mode of graphite, clearly stands out. This peak corresponds to the vibration of sp$^2$-hybridized carbon atoms in a two-dimensional hexagonal lattice. The fact that its intensity is significantly larger than that of the D band, is an indication of a high degree of sp$^2$ hybridization in the structure of the CDs.

For the further investigation of the functionalities found on the structure of the CDs their FT-IR spectra were obtained (Figure 6). Table 2 lists the main peaks and their assignments.

**Table 2: The main peaks and their assignments of the TTDDA solution, Arg TTDDA CDs, and arginine in water**

| TTDDA solution | Arg TTDDA CDs | Arginine in water | Assignment |
|---|---|---|---|
| 3363.19 | 3352.00 | 3328.39 | O-H symmetric stretching |
| | | 3148.21 | N-H stretching |
| 2927.70 | 2917.45 | 2951.42 | C-H asymmetric stretching of ($-CH_3$) |
| 2874.04 | 2867.78 | | C-H symmetric stretching of ($-CH_2$) |
| 1640.73 | 1630.4 | | C=C stretch, or COO-, or Amide I (1620-1680) C=O stretching vibration |
| | | 1612.95 | N-H bending |
| 1562.56 | 1560.19 | | Amide II (1510-1580) due both to N-H bending and C-N stretching vibrations |
| | | 1497.72 | N-H bending |
| 1483.02 | 1469.07 | | $\delta CH_2$ |
| | | 1403.66 | $COO^-$ stretching |
| 1389.81 | 1388.54 | | -C-H bending |
| 1349.64 | | 1344.55 | $CH_3$ symmetric bending |
| 1310.20 | 1305.46 | | C-N stretching |
| | | 1165.14 | C-C-C symmetric stretching |
| | | 1114.42 | C-O stretching |
| 1086.93 | 1087.68 | | C-O stretching in primary alcohols |

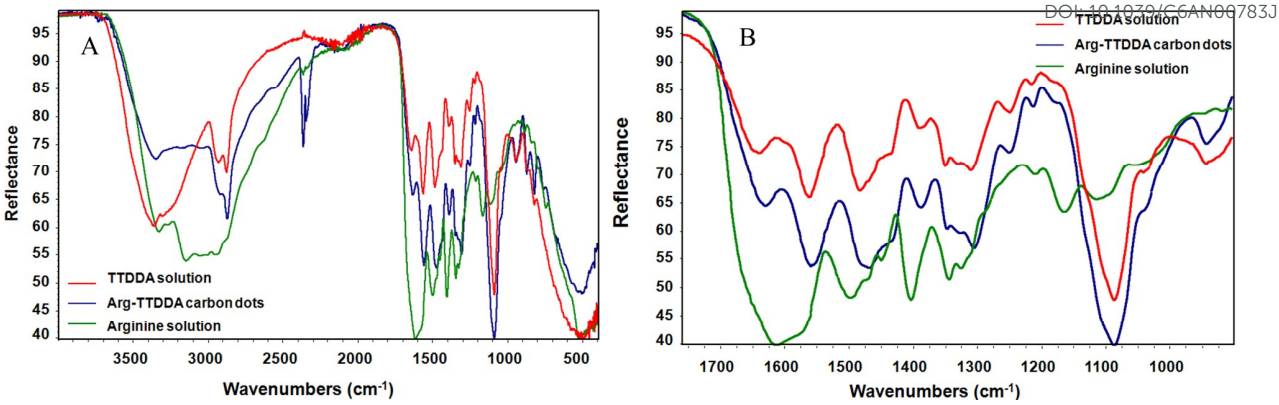


**Figure 6.** (a) FT-IR spectra of the TTDDA solution, Arg TTDDA CDs, and Arginine.

(b) A close up of the region containing the peaks of interest.

As observed from Figure 6b, the IR peaks of the arginine solution are not present in the CDs spectrum. This is attributed to the fact that during the microwave assisted pyrolisys procedure, arginine is used as the carbon source for the formation of the CDs, and it is thus completely consumed. If the spectra of the TTDDA solution and of the CDs are compared, it is observed that there is a shift in the two main peaks that appear in the region between 1500-1700cm$^{-1}$. The first peak, attributed to both N-H bending and C-N stretching vibrations (Amide II), shows a small shift of about 2cm$^{-1}$, moving from TTDDA (1562.56cm$^{-1}$) to CDs (1560.19cm$^{-1}$). The second peak, which is attributed to either the C=C stretch or COO- or Amide I C=O stretching vibration, shows a shift of 10cm$^{-1}$. While the TTDDA has a peak at 1640.73cm$^{-1}$, the CDs peak appears at 1630.4cm$^{-1}$. The observed shift is attributed to the insertion of the TTDDA molecules onto the surface of the newly formed CDs, which influences their vibration modes. From this data, it is concluded that during the synthesis of the CDs the arginine is used as the starting material and TTDDA as linker, thus producing nanoparticles functionalized with TTDDA moieties on their surface.

## The effect of pH and $H_2O_2$ on the CDs fluorescence

Since the surface of the synthesized CDs is composed of amino-terminated functionalities, we expect that a change in the surrounding pH will impose a change in the observed fluorescence. It is expected that there is going to be a shift either in the wavelength and/or the intensity the fluorescence spectrum. In order to verify the validity of this assumption, the fluorescence of the

CDs in solutions of different pH values and the response was monitored. The results are shown in Figure 7.

View Article Online
DOI: 10.1039/C6AN00783J

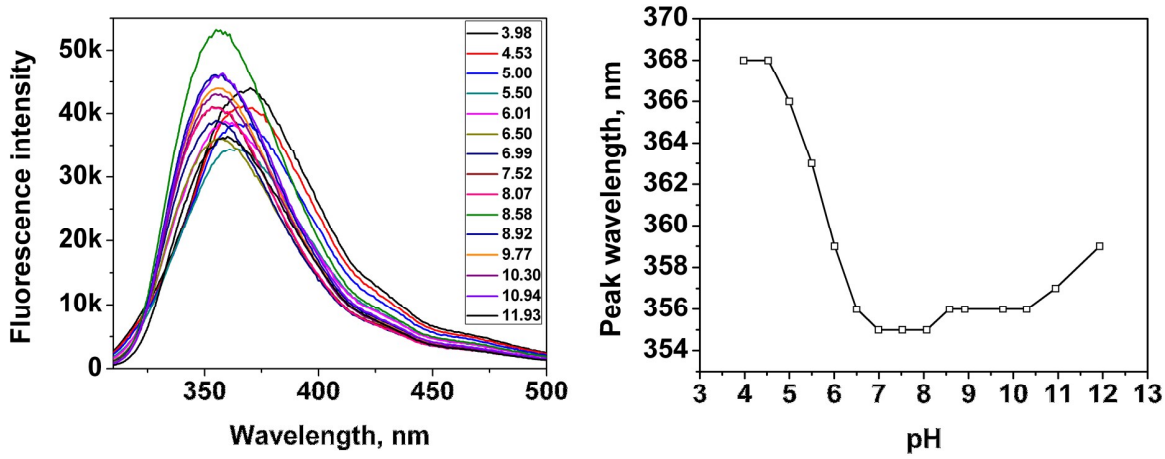


**Figure 7.** pH dependence of CDs (a), and the changes that the peak wavelength suffers (b). Excitation wavelength set at 325nm

Figure 7a shows the emission spectra of the CDs with solutions over a wide range of pH values. It is observed that the spectral features of the CDs change as the pH of the solution changes. It is shown that the emission peak, the wavelength, as well as the fluorescence intensity are affected by the changes in the pH values. Initially, as the pH decreases to the acidic region, the fluorescence intensity of the CDs shows a large blue shift from the initial peak from 368nm to 355nm, accompanied by a very large decrease of the fluorescence intensity. In the neutral and basic areas of the pH scale, the fluorescence intensity of the CDs shows a red shift returning to 359nm, with a concurrent increase in the peak intensity. These results indicate that any small pH change in the surrounding of the CDs does indeed affect the observed fluorescence, in a reversible manner.

Subsequently the effect of hydrogen peroxide on the observed fluorescence efficiency of the CDs was determined. For this purpose, the fluorescence of CDs was measured under a wide concentration range of hydrogen peroxide and the data is shown in Figure 8.

View Article Online
DOI: 10.1039/C6AN00783J

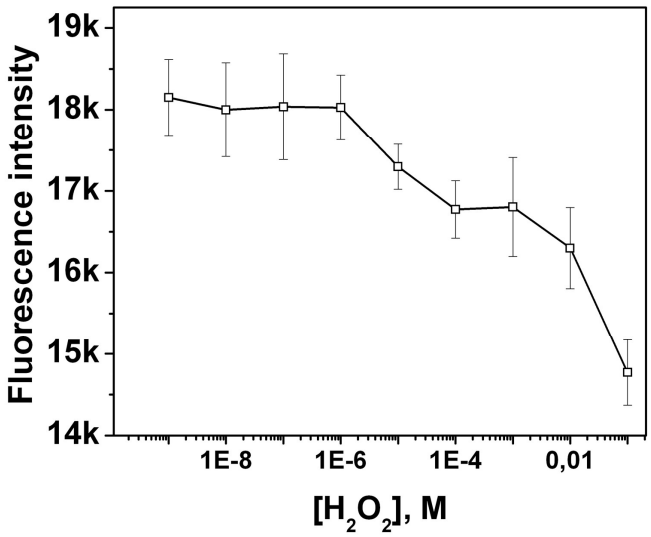


**Figure 8.** Dependence of the CDs fluorescence on the $H_2O_2$ concentration

We can clearly observe that at concentrations in the nanomolar range, the fluorescence signal of the CDs is not affected significantly. At these levels, the $H_2O_2$ concentration is either too low, or unstable with time to induce any effects. When the $H_2O_2$ concentration is in the micromolar range, the fluorescence signal of the CDs starts decreasing and continues to drop significantly as the $H_2O_2$ concentration increases. This indicates that a similar response should be expected from the GOx – CDs complexes to be further constructed and used in experiments, with their fluorescence decreasing with increase of the $H_2O_2$ concentration in the system.

In order to verify that the fluorescence decrease observed upon addition of $H_2O_2$ is due solely to its effect on the amino groups surrounding the CDs and it is not an artifact, the absorbance spectra of the CDs with and without $H_2O_2$ was recorded. As can be seen from Figure 9, there is no difference between the spectra, indicating that the changes recorded in the fluorescence of the dots upon additions of $H_2O_2$ are due to the changes produced in the pH value of the surrounding environment and not to other sources.

View Article Online
DOI: 10.1039/C6AN00783J

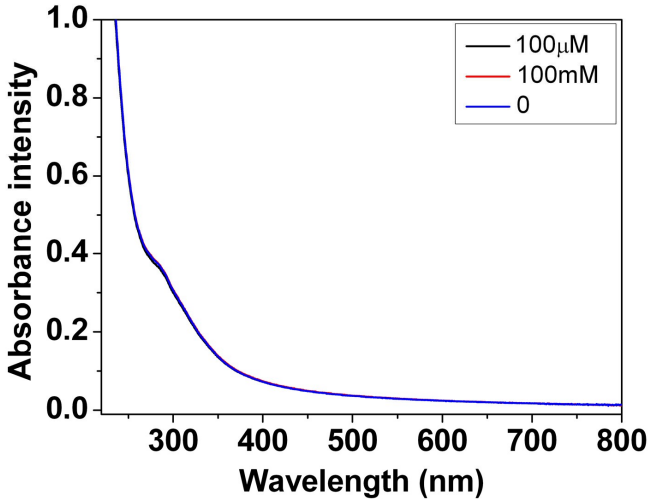


**Figure 9.** Absorbance spectra of CDs with and without $H_2O_2$ (final concentrations in solution).

## Use of CDs for optical biosensor development

It is well known that many enzyme catalyzed reactions produce, amongst others, peroxide, acidic or basic products. Since the effect of changes on either the pH or the peroxide surrounding the CDs is expected to have a strong influence on the PL properties of the CDs, they are considered useful for the development of such detection systems. For this reason, we have used in this study a well known enzymatic reaction based on GOx, which upon hydrolysis of glucose produces hydrogen peroxide and D-glucono δ lactone as it is shown in the following equation:

$$\text{Glucose} + O_2 \xrightarrow{\text{GOx}} \text{D Glucono } \delta \text{ lactone} + H_2O_2$$

Eq. 1

This fact, together with the previous results of pH and peroxide effect on the fluorescence spectra of the CDs, indicate that GOx immobilized onto the surface of the CDs is a valid platform for the development of the biosensors (Figure 10)

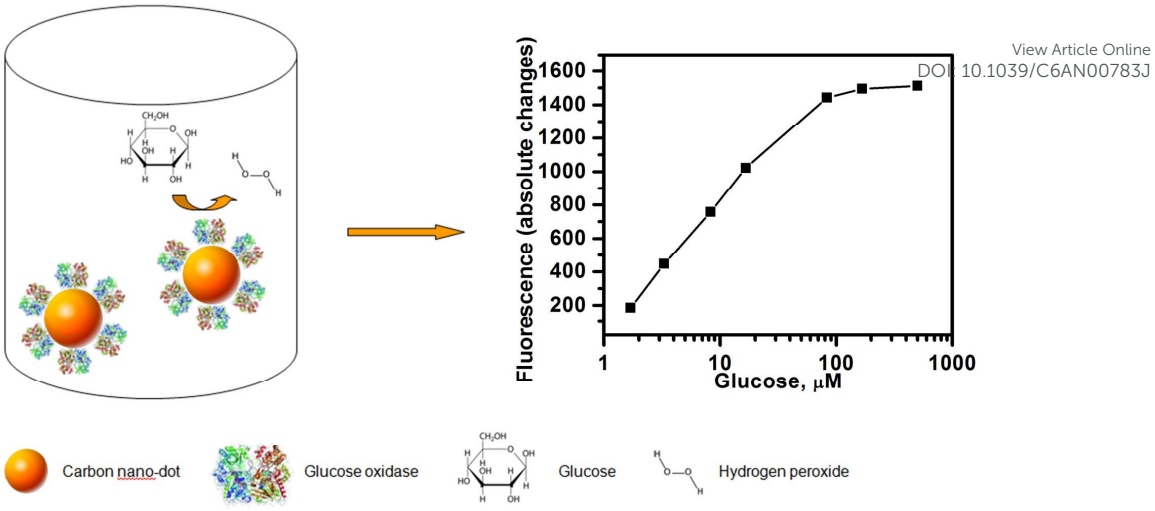


**Figure 10.** Schematic representation of the biosensors' operation

The newly synthesized CDs are tested for their response to glucose in order to determine whether its presence produces changes in the fluorescence spectrum or the fluorescence intensity of the CDs. For this purpose, the CDs were mixed with different quantities of glucose to a final concentration between 1nM and 100mM, as can be seen from Figure 11. It is observed that the addition of various amounts of glucose, even at very high concentrations (100mM), does not affect the fluorescence of our newly synthesized CDs. This is due to the fact that the glucose molecule does not have functional groups that could interact with the amino-groups found on the surface of the CDs, determining a disturbance of their fluorescence signal.

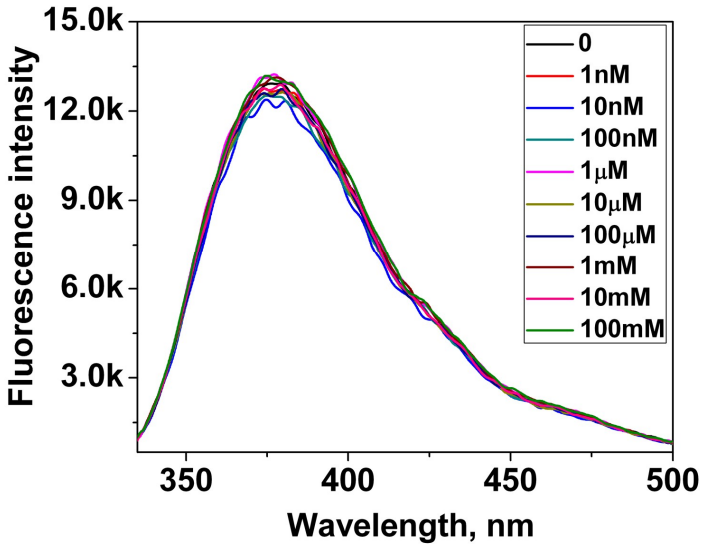


**Figure 11.** CDs response to glucose (final concentrations in solution)

Conventional gel electrophoresis allows for the separation of protein samples according to their molecular masses. This way we have investigated the immobilization of the enzyme onto the surface of the CDs. The difference in the molecular weight of the free CDs and of the GOx – CD is obvious. Specifically, it is easily observed that the free enzyme (Figure 12, Lane 2) has a lower molecular weight resulting in a higher migration and appearing lower in comparison to the immobilized GOx. The GOx - CDs complex, due to a higher total molecular weight (Lane 3) migrated less while the free CDs (Lane 1) do not present any characteristic band as enzymes and proteins do, and appear as a broad area at lower molecular weights.

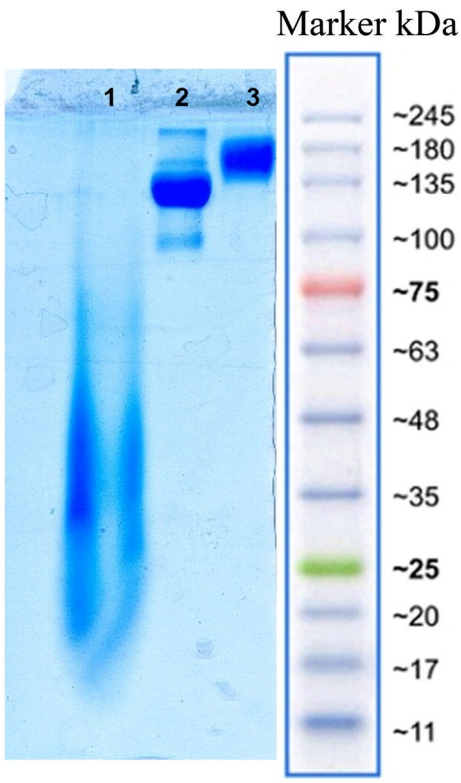


**Figure 12.** Electrophoresis of CDs, GOx and CDs – GOx complex

It is worth noting that the conjugation of GOx onto the surface of CDs does not produce modifications in the shape of their fluorescence curve.

The kinetic behavior of the GOx was studied before and after immobilization and from the diagrams of 1/V via 1/S for the free and immobilized GOx, the kinetic parameters $V_{max}$ and $K_m$ (Michaelis Menten constant) were determined according to the corresponding Michaelis–Menten equation. The data is presented in Table 3.

It is clearly seen that the immobilization of GOx onto the surface of the CDs does not produce a change in the $K_m$ value. This is an indication that the immobilization process does not result in a

modification of the affinity of the enzyme to its substrate, binding it equally efficient. On the other hand, the $V_{max}$ of the GOx registers a decrease of about 80% after immobilization, which is probably due to diffusion restrictions of the substrate and interactions with the CDs.

**Table 3. Kinetic parameters of free and CDs – GOx**

| Kinetic Parameters | $K_m$ [M] | $V_{max}$ [1/s] |
|---|---|---|
| GOx | 0.173 | 12.791 |
| CDs - GOx | 0.173 | 2.620 |

After immobilization of the enzyme onto the surface of the CDs, the response of the CDs – GOx complex to the substrate glucose (Glu) was evaluated (Figure 13a and 13b). Upon a careful examination of Figure 13a, it is observed that there is a significant change of CDs fluorescence upon addition of Glu in the micromolar range, the larger the concentration of Glu is, the higher the decrease in the registered fluorescence of the CDs. On the other hand, there is no significant change in the nanomolar range. We believe that with increasing the concentration of Glu, the enzymatic reaction produces larger quantities of $H_2O_2$, which then result in perturbations of the environment surrounding the CDs and changes of pH. This is backed also by the results presented previously, where changes in the pH of the surrounding environment of the CDs produced changes in their fluorescence intensity.

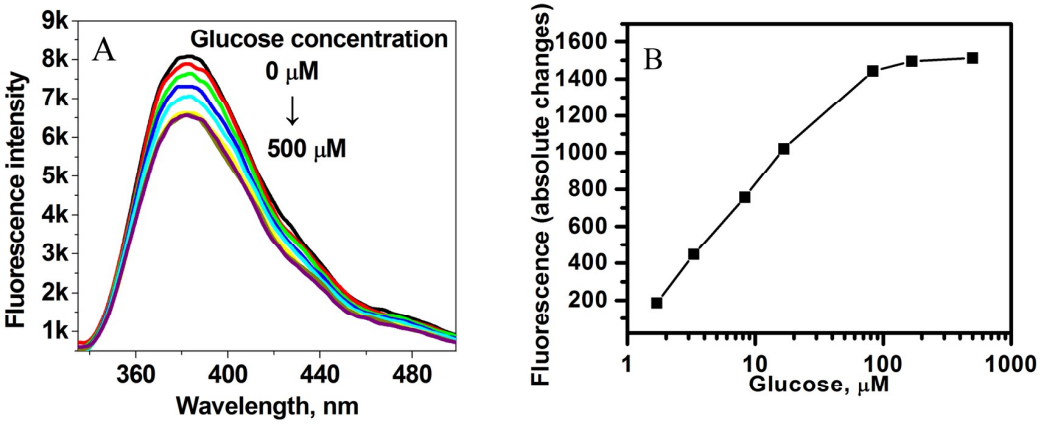


**Figure 13.** (a) Response of the CDs – GOx complex to the formation of $H_2O_2$ through the enzymatic reaction of glucose (final glucose concentrations in solution). (b) Calibration curve of the CDs – GOx biosensor (logarithmic scale).

The experiment was performed with a large scale of substrate concentrations (1.7 – 500μM), and as can be seen from Figure 13b, the system presents a linear relationship between the concentration of the substrate and the enzyme activity at substrate concentrations below 100μM with a detection limit of 1.17μM which is in the same range as another literature report[54].

## *CONCLUSIONS*

The detailed characterization of synthetic CDs has been presented, as a basis for the development of a biosensor platform. Based on the results of spectroscopic analyses, we have shown that CDs are useful and unique tools for fluorescent based biosensor development. The synthesis of CDs employed in this work is rapid, facile, repeatable, and provides us with particles easily functionalizable with biomolecules due to the presence of amino functional groups on their surface. These surface amino functionalities render the CDs sensitive to proton and peroxide concentration changes. As a model system, we examined the use of GOx, covalently attached to the surface of the CDs for the construction of CDs – GOx complex and the development of an optical biosensor. The enzymatic reaction affects the surface chemistry of the CDs, leading to large and reversible changes in their fluorescence intensity. The observed changes in the fluorescence signal are directly related with the substrate's concentration in the solution. In this way we have demonstrated the efficacy of a new highly sensitive biosensing system of glucose based on fluorescent CDs.

## *ACKNOWLEDGMENT*

This study was financially supported by the Greek "ARISTEIA II" Action of the "OPERATIONAL PROGRAMME EDUCATION AND LIFELONG LEARNING" and is co-funded by the European Social Fund (ESF) and National Resources.

## *REFERENCES*

[1] R. C. Somers, M. G. Bawendi and D. G. Nocera, *Chem. Soc. Rev.*, 2007, **36**, 579-591.

[2] M. Frasco, V. Vamvakaki and N. A. Chaniotakis, *J. Nanopart. Res.*, 2010, **12**, 1449-1458.

[3] M. C. Daniel and D. Astruc, *Chem. Rev.*, 2004, **104**, 293-346.

[4] V. Vamvakaki, M. Fouskaki and N. A. Chaniotakis, *Anal. Lett.*, 2007, **40**, 2271-2287.

[5] G. A. Crespo, S. Macho, J. Bobacka and F. X. Rius, *Anal. Chem.*, 2009, **81**, 676-681.

[6] Y. P. Sun, B. Zhou, Y. Lin, W. Wang, K. A. Shiral Fernando, P. Pathak, M. J. Meziani, B. A. Harruff, X. Wang, H. Wang, P. G. Luo, H. Yang, M. E. Kose, B. Chen, L. M. Veca and S. Y. Xie, *J. Am. Chem. Soc.*, 2006, **128**, 7756-7757.

[7] J. Zhou, C. Booker, R. Li, X. Zhou, T. K. Sham, X. Sun and Z. Ding, *J. Am. Chem. Soc.*, 2007, **129**, 744-745.

[8] Q. L. Zhao, Z. L. Zhang, B. H. Huang, J. Peng, M. Zhang and D. W. Pang, *Chem. Commun.*, 2008, **41**, 5116-5118.

[9] S. Baker and G. A. Baker, *Angew. Chem. Int. Ed.*, 2010, **49**, 6726 – 6744.

[10] L. Cao, X. Wang, M. J. Meziani, F. Lu, H. Wang, P. G. Luo, Y. Lin, B. A. Harruff, L. M. Veca, D. Murray, S. Y. Xie and Y. P. Sun, *J. Am. Chem. Soc.*, 2007, **129**, 11318-11319.

[11] A. B. Bourlinos, A. Stassinopoulos, D. Anglos, R. Zboril, M. Karakassides and E. P. Giannelis, *Small*, 2008, **4**, 455-458.

[12] L. Zheng, Y. Chi, Y. Dong, J. Lin and B. Wang, *J. Am. Chem. Soc.*, 2009, **131**, 4564-4565.

[13] H. Liu, T. Ye and C. Mao, *Angew. Chem. Int. Ed.*, 2007, **46**, 6473-6475.

[14] G. A. Posthuma-Trumpie, J. H. Wichers, M. Koets, L. B. J. M. Berendsen and A. van Amerongen, *Anal. Bioanal. Chem.*, 2012, **402**, 593–600.

[15] J. C. G. E. da Silva and H. M. R. Gonçalves, *Tr. Anal. Chem.*, 2011, **30**, 1327-1336.

[16] Q. Li, T. Y. Ohulchanskyy, R. Liu , K. Koynov, D. Wu, A. Best, R. Kumar, A. Bonoiu, P. N. Prasad, *J. Phys. Chem. C,* 2010, **114**, 12062-12068

[17] A. Salinas-Castillo, M. Ariza-Avidad, C. Pritz, M. Camprubi-Robles, B. Fernandez, M. J. Ruedas-Rama, A. Megia-Fernandez, A. Lapresta-Fernandez, F. Santoyo-Gonzalez, A. Schrott-Fischer, L. F. Capitan-Vallvey, *Chem. Commun.,* 2013, **49**, 1103-1105

View Article Online
DOI: 10.1039/C6AN00783J

[18] X. Liu, N. Zhang, T. Bing, D. Shangguan, *Anal. Chem.,* 2014, **86**, 2289-2296

[19] P. Shen, Y. Xia, *Anal. Chem.,* 2014, **86** , 5323-5329

[20] Q. Wang, X. Huang, Y. Long, X. Wang, H. Zhang, R. Zhu, L. Liang, P. Teng, H. Zheng, *Carbon,* 2013, **59**, 192-199

[21] H. U. Lee, S. Y. Park, E. S. Park, B. Son, S. C. Lee, J. W. Lee, Y.-C. Lee, K. S. Kang, M. I. Kim, H. G. Park, S. Choi, Y. S. Huh, S.-Y. Lee, K.-B. Lee, Y.-K. Oh, J. Lee, *Sci. Rep.,* 2014, **4**, 4665

[22] P. Huang, J. Lin, X. S. Wang, Z. Wang, C. L. Zhang, M. He, K. Wang, F. Chen, Z. M. Li, G. X. Shen, D. X. Cui, X. Y. Chen, *Adv.Mater.,* 2012, **24**, 5104-5110

[23] B. R. Bitner, D. C. Marcano, J. M. Berlin, R. H. Fabian, L. Cherian, J. C. Culver, M. E. Dickinson, C. S. Robertson, R. G. Pautler, T. A. Kent, J. M. Tour, *ACS Nano,* 2012, **6**, 8007-8014

[24] S. Zhu, Y. Song, X. Zhao, J. Shao, J. Zhang and B. Yang, *Nano Res*., 2015, **8(2)**, 355-381.

[25] H. Li, X. He, Z. Kang, H. Huang, Y. Liu, J. Liu, S. Lian, C. H. A. Tsang, X. Yang and S. T. Lee, *Angew. Chem. Int. Ed.*, 2010, **49**, 4430-4434.

[26] M. J. Krysmann, A. Kelarakis, P. Dallas and E. P. Giannelis, *J. Am. Chem. Soc.*, 2012, **134**, 747-750.

[27] J. Peng, W. Gao, B. K. Gupta, Z. Liu, R. Romero-Aburto, L. Ge, L. Song, L. B. Alemany, X. Zhan, G. Gao, S. A. Vithayathil, B. A. Kaipparettu, A. A. Marti, T. Hayashi, J. J. Zhu and P. M. Ajayan, *Nano Lett.*, 2012, **12**, 844-849.

[28] X. Yan, B. Li, X. Cui, Q. Wei, K. Tajima and L. S. Li, *J. Phys. Chem. Lett.*, 2011, **2**, 1119-1124.

[29] C. Liu, P. Zhang, F. Tian, W. Li, F. Lib and W. Liu, *J. Mater. Chem.*, 2011, **21**, 13163-13167.

[30] K. E. Sapsford, T. Pons, I. L. Medintz and H. Mattoussi, *Sensors*, 2006, **6**, 925-953.

[31] T. Pellegrino, S. Kudera, T. Liedl, A. M. Javier, L. Manna and W. J. Parak, *Small*, 2005, **1**, 48-63.

[32] L. Agüí, P. Yáñez-Sedeño and J. M. Pingarrón, *Anal. Chim. Acta*, 2008, **622**, 11-47.

[33] W. Yang, P. Thordarson, J. J. Gooding, S. P. Ringer and F. Braet, *Nanotechnology*, 2007, **18**, 1-12.

View Article Online
DOI: 10.1039/C6AN00783J

[34] Y. Wang, S. Kalytchuk, Y. Zhang, H. C. Shi, S. V. Kershaw and A. L. Rogach, *J. Phys. Chem. Lett.*, 2014, **5**, 1412–1420.

[35] W. L. Wilson, P. F. Szajowski and L. E. Brus, *Science*, 1993, **262**, 1242-1244.

[36] H. P. Liu, T. Ye and C. D. Mao, *Angew. Chem. Int. Ed.*, 2007, **46**, 6473-6475.

[37] R. L. Liu, D. Q. Wu, S. H. Liu, K. Koynov, W. Knoll and Q. Li, *Angew. Chem. Int. Ed.*, 2009, **48**, 4598-4601.

[38] H. T. Li, H. Ming, Y. Liu, H. Yu, X. D. He, H. Huang, K. M. Pan, Z. H. Kang and S. T. Lee, *New J. Chem.*, 2011, **35**, 2666-2670.

[39] A. Philippidis, D. Stefanakis, D. Anglos and D. Ghanotakis, *J. Nanopart. Res.*, 2013, **15**:1414.

[40] P. C. Lee and D. Meisel, *J. Phys. Chem.,* 1982, **86**, 3391-3395.

[41] M. M. Bradford, *Anal. Biochem.*, 1976, **72**, 248–254.

[42] U. K. Laemmli, *Nature*, 1970, **227**, 680 – 685.

[43] C. Lanzellotto, G. Favero, M.L. Antonelli, C. Tortolini, S. Cannistraro, E. Coppari and F. Mazzei, *Biosens. Bioelectron*., 2014, **55**, 430-437.

[44] K. Saeedfar, L. Y. Heng, T. L. Ling and M. Rezayi, *Sensors* 2013, **13**, 16851-16866.

[45] Q. Wang, Q. Li, X. Yang, K. Wang, S. Du, H. Zhang and Y. Nie, *Biosens. Bioelectron*., 2016, **77**, 1001–1007.

[46] M. Veerapandian1, Y.Seo, H. Shin, K. Yun and M.H. Lee, *Int. J. Nanomed*., 2012, **7**, 6123–6136.

[47] A. I. Gopalana,b, K.P. Lee and D. Ragupathy, *Biosens. Bioelectron*., 2009, **24**, 2211–2217.

[48] S. Palanisamy, S. Cheemalapati and S. M. Chen, *Mat. Sci. Eng. C*, 2014, **34**, 207–213.

[49] D.L. Dexter, *J. Chem. Phys*., 1953, **21**, 836-850

[50] T. Takagahara and K. Takeda, *Phys. Rev. B,* 1992, **46**, 15578R.

[51] M. Inokuti and F. Hirayama, *J. Chem. Phys*., 1965, **43**, 1978-1989

[52] A. C. Ferrari and J. Robertson, *Phys. Rev. B*., 2000, **61**, 15095-14107.

[53] N. D. T. Parab and V. Tomar, *J. Nanomed. Nanotechnol*., 2012, **3(2)**, 131

[54] P. Shen and Y. Xia, *Anal. Chem*., 2014, **86**, 5323-5329